This article has been accepted for publication in IEEE Antennas and Propagation Magazine. This is the author's version which has not been fully edited and content may change prior to final publication. Citation information: DOI 10.1109/MAP.2024.3362249

Roger F. Harrington and the Method of Moments; Part I: Electrostatics

J. R. Mosig, Life Fellow, IEEE

Ecole Polytechnique Fédérale de Lausanne (EPFL), Switzerland, CH-1015, Lausanne, Switzerland

Abstract: The Method of Moments, as introduced by R.F. Harrington more than 50 years ago, is reviewed in the context of the classic potential integral equation formulations applied to both electrostatic (part-I) and electrodynamic or full-wave problems (part-II). A systematic treatment is presented, based on the concept of "discrete Green's functions". For the sake of simplicity and clarity, the developments are restricted to geometries composed of 2D metallic plates embedded in a homogeneous medium. Within this framework, original analytical developments are presented. They simplify the formulations and enable the implementation of Point-Matching and Galerkin strategies without any need for a numerical evaluation of the involved multidimensional integrals. Simple MatLab codes are provided, allowing the reader not only to reproduce but also to go beyond the pioneering results of Harrington, to whom this paper pays an undisguised homage.

Index Terms: Integral equations, Method of moments, Galerkin, Point-Matching, multidimensional integrals, capacitances, condensers

1. Introduction

More than 50 years ago, in 1968, a book was published that would change forever the numerical approaches used in computational electromagnetics and, more specifically, in antenna and microwave engineering. Its title was “Field Computation by Moment Methods” [1] and its author, Roger F. Harrington, was then a young professor at Syracuse University, NY, USA. As Prof. Harrington himself explained in a very illuminating paper [2] about the history of the genesis of his book, the name “Method of Moments” (MoM) was selected because this was the name used by the Russian mathematicians Kantorovich and Akilov [3] for a similar method in the realm of functional analysis.

Since its publication, this book has become one of the most cited in our domain (at the moment of writing, Google Scholar mentions almost 13'000 citations) and the number of research papers using the method of moments is overwhelming. A good compilation of early MoM papers can be found in the book “Computational Electromagnetics”, subtitled “Frequency Domain Method of Moments” [4]. In the wake of Harrington’s book, several books have been published, generalizing the MoM and applying it to highly diverse problems (see for instance [5], recently enlarged and reissued). However, this author firmly believes that “Field Computation” remains the best possible introduction to the method.

In 1968, Prof. Harrington was already a well-known figure in our community, after having published in 1961 another landmark book, “Time-Harmonic Electromagnetic Fields” [6]. Despite this fact, his method of moments was not immediately accepted by the specialists. A well-known story, related by Don Wilton [7], tells us that the 1967 Proceedings of the IEEE paper [8], anticipating his book and containing a summary of it, had been previously rejected by the IEEE TAP journal. Reviewers had argued against the possibility of representing continuous quantities, such as electric currents, using discontinuous quantities and against the possibility of inverting a 100 x 100 matrix in a computer, “because the magnetic tape unit would wear out going back and forth”. Times have changed.

In a retrospective paper [9], Jim Rautio, a former student of Harrington, tells us how the 100 unknown barrier was broken in 1982 by using one of the first IBM PCs rated at 4.77 MHz (!) (solving the linear system took one hour...) and how twenty years later, he was customarily doing in about two hours direct matrix solutions of linear systems with one hundred thousand unknowns, using another IBM PC rated at 2.4 GHz.

Clearly, the amazing increase in computer speed and memory in the last 40 years is one reason for the popularity of MoM. But we must not neglect the outstanding abilities of Prof. Harrington as a scientific writer in the engineering realm. In his two books [1, 6], the mathematical language is as simple as possible, while remaining rigorous. The treatment is always guided by the physical interpretation of the subject, and approximations are not ignored if they result in a reasonable trade-off between the complexity of analytical developments and the accuracy of the results. It is no surprise that these books are electrical engineering best-sellers.

MoM is a general strategy for solving any linear operator equation and allows us to numerically solve any linear electromagnetic boundary value problem arising from Maxwell's equations [7]. Here we want to pay homage to Harrington's work and to highlight his achievements by reviewing the MoM formulation for potential-based integral equations. We then revisit some of the simple canonical geometries he studied, using a generalized strategy. This paper is in two parts dealing, respectively, with electrostatic and electrodynamic (time-harmonic full-wave) situations.

2. The Potential Integral Equation for metallic bodies

Consider an ideal metallic body (perfect electric conductor) illuminated by a known excitation electric field, which can be also expressed as an excitation potential, with the classical relationship $\mathbf{E_{exc}} = -\nabla V_{exc}$.

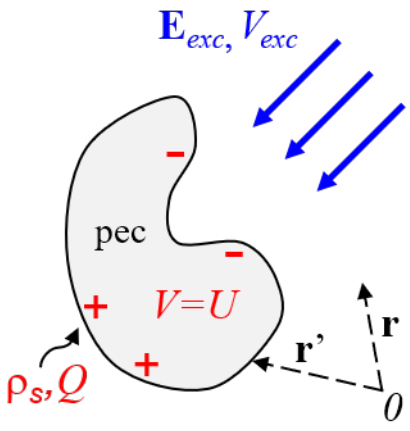

Figure 1: An excitation electric field $\mathbf{E_{exc}}$ creates a surface charge density ρ_s on a perfect electric conductor body. The body may have a total non-zero charge Q. The electrostatic potential of the body U can be known and imposed by external circumstances (battery-connected or grounded body) or unknown, to be determined (isolated body). But in all cases, it remains constant inside the body and on its surface.

As a result of this excitation (Fig. 1), an unknown surface charge density ρ_s appears on the surface of the body. This charge produces in turn an "induced" electric field/potential (in electrodynamics, the adjective "induced" will be replaced by "scattered"). Basic electrostatic theory tells us that the induced potential at an observation point $\mathbf{r}$ can be expressed as:

$$4\pi\varepsilon_0 V_{ind}(\mathbf{r}) = \int_S ds'\, \rho_s(\mathbf{r'}) G(\mathbf{r}\,|\,\mathbf{r'}) = G \otimes \rho_s \qquad (1)$$

Here $G(\mathbf{r}\,|\,\mathbf{r'})$ is the pertinent Green's function (GF) and the convolution notation $\otimes$ has been introduced (in free space $G(\mathbf{r}\,|\,\mathbf{r'}) = 1/|\,\mathbf{r}-\mathbf{r'}\,|$).

The physics of the problem requires that the induced potential "compensates" the excitation potential producing a total potential U, not necessarily known but constant on the body's surface. This condition allows us to set up a potential integral equation (PIE) for the unknown surface charge density ρ_s which

can be written in compact notation as:

$$G \otimes \rho_s = 4\pi\varepsilon_0 (U - V_{exc}) \tag{2a}$$

The total charge on the body's surface is then given by: $Q = \int_S ds\, \rho_s$ (2b)

In general, either the body has a known potential U (being connected to a battery or grounded) or it has a known total charge Q (isolated body). In the first situation, the total charge is unknown but can be computed a posteriori using (2b). In the second situation, (2b) provides a supplementary equation allowing us to deal with the additional unknown U. Obviously, in absence of an external excitation $(V_{exc} = 0)$, the set of equations (2) can have a non-zero solution for ρ_s only if either U or Q have non-zero values. In the next section, we will set up some possible solutions of this PIE using the MoM.

3. MoM solution: subsectional basis functions and discrete Green's functions

This section deals with some classical developments, fully covered in Harrington's book [1, sections 1.3 to 1.5 and 2.1 to 2.2]. Here, for the sake of completeness, we briefly revisit the formulation using a slightly different point of view. The MoM transforms the PIE (2) into a linear algebraic system by expanding the unknown charge density into a set N basis functions b_j as:

$$\rho_s = \sum_{j=1}^{N} \alpha_j b_j \tag{3}$$

where α_j are constant expansion coefficients to be determined. Then, the integral equation is projected into a set of test functions t_i with the help of a predefined inner product [1, sect. 1.2], denoted by $\langle\ \rangle$ and defined here as:

$$\langle t_i, f \rangle = \int_{S_i} ds\, t_i(\mathbf{r}) f(\mathbf{r}) \tag{4}$$

The resulting matrix equation can be written as:

$$[c_{ij}][\alpha_j] = [e_i] \tag{5a}$$

The most commonly used basis and test functions are "subsectional" functions which exist only over subsections ("cells") S_i of the integration domain S ([1], sect. 1.5). In this paper, we will only use these functions. With these assumptions, the MoM matrix elements are given by:

$$c_{ij} = \langle t_i, G \otimes b_j \rangle = \int_{S_i} ds\, t_i(\mathbf{r}) \int_{S_j} G(\mathbf{r} \mid \mathbf{r}') b_j(\mathbf{r}') \tag{5b}$$

and the excitation vector elements by:

$$e_i = 4\pi\varepsilon_0 \langle t_i, U - V_{exc}(\mathbf{r}) \rangle = 4\pi\varepsilon_0 \int_{S_i} ds\, t_i(\mathbf{r}) [U - V_{exc}(\mathbf{r})] \tag{5c}$$

Quite frequently, we select the same functions for basis and test, $t_i = b_i$. This is the Galerkin method, endowed with interesting variational properties [1, sect. 1.8].

In electrostatic problems dealing with surfaces, the simplest possible subsectional basis, used by Harrington, is the piecewise constant basis, mathematically defined as a 2D-pulse function Π existing over a subsection (cell) of the problem. The pulse amplitude is selected to have either a unit surface charge density or a unit total cell charge. For reasons that will become soon evident, we will favor this second choice, which results in the definition:

$$b_j(\mathbf{r}') = \frac{1}{S_j}\Pi(S_j) \;\; ; \;\; \Pi(S_j) = \begin{cases} 1 & \text{if } \mathbf{r}' \in S_j \\ 0 & \text{elsewhere} \end{cases} \tag{6}$$

We now will specialize the Galerkin implementation (5) to these basis functions.

The writing of the final expressions is greatly simplified by the introduction of the so-called "discrete GFs" and "averaged discrete GFs". While a GF has always a point source, the discrete GF, Γ_{ij}, is obtained when a full basis function is used as source and can be mathematically expressed as:

$$\Gamma_{ij} = \Gamma(\mathbf{r}_i, S_j) = \frac{1}{S_j}\int_{S_j} ds'\, G(\mathbf{r}_i \,|\, \mathbf{r}') \tag{7a}$$

where $\mathbf{r}_i$ denotes the center of the test cell S_i .

In a subsequent step, we consider the mean value of a discrete GF when the observer point spans a test cell S_i. This is the averaged discrete GF Ψ_{ij} given by:

$$\Psi_{ij} = \Psi(S_i, S_j) = \frac{1}{S_i}\int_{S_i} ds\, \Gamma(\mathbf{r}, S_j) = \frac{1}{S_i S_j}\int_{S_i} ds \int_{S_j} ds'\, G(\mathbf{r} \,|\, \mathbf{r}') \tag{7b}$$

In other words, the discrete GF is a "basis-integrated GF", given by the mean value of the corresponding GF when the source point spans a basis cell S_j. And the averaged discrete GF is the "basis&test integrated GF", given by mean value of the corresponding discrete GF when averaged over a test cell. With this notation, the elements of the MoM-Galerkin linear system (5) can be simply written as:

$$c_{ij} = \Psi(S_i, S_j) \;; \;\; e_i = 4\pi\varepsilon_0 \frac{1}{S_i}\int_{S_i} ds\, [U - V_{exc}(\mathbf{r})] \tag{8}$$

The averaged discrete GFs, given by double surface integrals, can be approximated at different levels of accuracy. First, we can use the Mean Value Theorem of integral calculus to evaluate the testing integrals (on the observer's $\mathbf{r}$ coordinates). This amounts to replacing the averaged discrete GF by a discrete GF computed at the center of the test cell; then (8) can be approximated as:

$$c_{ij} \simeq \Gamma(\mathbf{r}_i, S_j) \;\; ; \;\; e_i \simeq 4\pi\varepsilon_0 [U - V_{exc}(\mathbf{r}_i)] \tag{9}$$

The same result (9) could have been formally obtained by using Dirac's delta functions as test functions. This was the approach taken by Harrington, resulting in the MoM implementation which he called "point-matching" ([1], sect. 1.4). The name is fully justified, because the point-matching (PM) approach boils down to satisfying the PIE (2) only at a set of discrete points (the cells' centers), where the potential created by the basis functions must be calculated.

In a further simplification, the Mean Value Theorem is applied again, this time to the source integral. The result reduces the MoM matrix elements to simply the value of the GF evaluated at the centers of test and basis cells. This will be called the "Green's function approximation:

$$c_{ij} \simeq G(\mathbf{r}_i \,|\, \mathbf{r}_j) \tag{10}$$

Because of the singularity of our GF, this bold simplification cannot obviously be applied to the diagonal terms c_{ii} , but it will provide a first-order approximation if $i \neq j$.

In practice, approximations of different levels can be mixed when filling the MoM matrix, trying to achieve the best trade-off between simplicity of the analytical developments, computer time, and accuracy of the results. After all, as noted above, all the possible combinations can be considered as numerical approximations of the original Galerkin formulation [10].

For instance, a reasonable Galerkin implementation can use the rigorous expressions (8) only for the self-interactions and possibly for the interaction between adjacent cells, while computing all the remaining matrix elements with the approximations (9) or (10). In his book, Harrington frequently used a PM formulation (9), but with a liberal use of the drastic approximation (10), which was applied

everywhere but in the diagonal elements ([1], eqn. 2.32). Now, we see clearly the benefits of our choice (6) for the basis functions. The MoM elements in the different approaches (8-10) are always given by GF values, possibly averaged over the cells' surfaces. This provides an easy check of the implementations and allows a direct comparison between the different MoM versions.
In the next sections, we will review and complete some of Harrington's developments for the canonical case of parallel rectangular plates in free space.

4. Analytical results for parallel rectangular cells in free space

In his electrostatic examples, Harrington always considered free-space situations, allowing him to use the free-space GF $G(\mathbf{r}\,|\,\mathbf{r}') = 1/|\,\mathbf{r}-\mathbf{r}'\,|$. And he always used a Point-Matching approach, approximating his surfaces by a set of square cells with constant surface charge (subareas, as he called them), even in the case of a hollow conducting cylinder [1, sect.2.3]. While all these restrictions were fully justified, taking into account the limited computational resources of his time, nowadays it is customary to consider more sophisticated choices like, for instance, Galerkin strategies using linear basis functions defined on triangular cells. In our community, this has been mostly done in the frame of scattering and antenna problems, where a frequency-dependent Green's function is needed. Therefore, we will delay the discussion of this subject until the second part of this paper, dealing with Electrodynamics problems.
Harrington never considered a real application of the Galerkin approach in his book [1]. This is likely due to the fact that the analytical calculation of the generic 4D integrals (5b) is a formidable task. As for a purely numerical evaluation, this was probably not feasible in the seventies and remains today a time-consuming task. On the other hand, a full analytical solution can be obtained for rectangular cells in free space, at least for some specific situations that include parallel and orthogonal orientations, although the complexity of the final formulas can be discouraging. See [11] for pioneering work and [12] for a recent more comprehensive study.
In this paper, we will pursue a more modest goal, limiting ourselves to a Galerkin formulation using piecewise constant functions defined on rectangular grids placed on parallel planes and sharing a common orientation. This generalization of Harrington's procedures will be enough to ascertain the accuracy he reached, while allowing the study of other interesting problems, like stacked parallel plates of different sizes. We will consider uniform meshes with identical cells, all of dimensions $a \times b$.

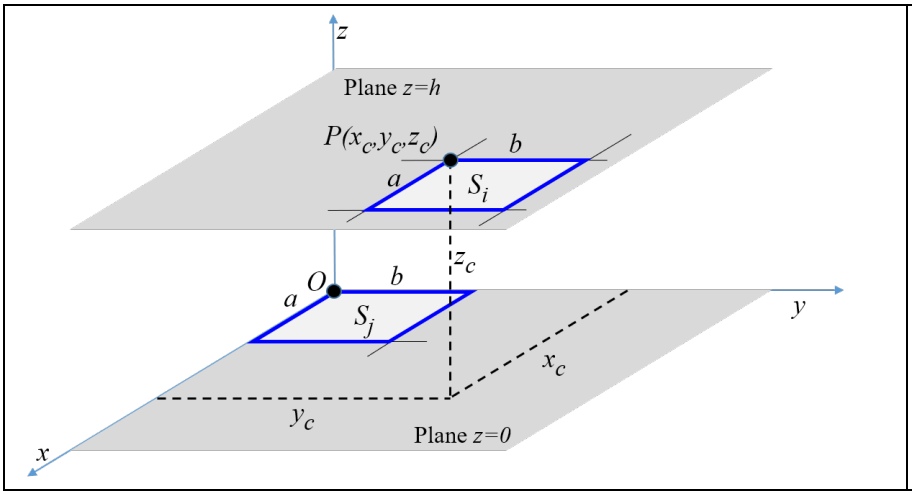

Figure 2: Basis and test cells of equal size and orientations and located in parallel planes. A corner of the basis cell is centered at the origin of coordinates. The coordinates of the test cell's corresponding corner are (x_c, y_c, z_c)

In general, the j-th basis cell has its center at (x_j, y_j, z_j) and the i-th test cell center is at (x_i, y_i, z_i). We can always make a coordinate translation to put the lower left corner of the basis cell at the origin of coordinates. Then, as depicted in Fig.2, the lower left corner of the test cell is at (x_c, y_c, z_c) with $x_c = |\,x_i - x_j\,|$, $y_c = |\,y_i - y_j\,|$ and $z_c = |\,z_i - z_j\,|$. Notice that due to the symmetry of the GFs, we

can assume x_c and y_c as being always positive. As for the third coordinate, we will simply write $z_c = |z_i - z_j| = h$. With this notation we make it clear that, since we will only consider plates parallel to the *xy*-plane, the *z*-coordinates are never variables of integration but take a constant value h, which is simply the vertical distance between the plates (obviously $h = 0$ if the i-th and j-th cells belong to the same plate).

Then, for plates embedded in free space, the MoM matrix elements c_{ij} in (8) are given by:

$$c_{ij} = \Psi(S_i, S_j) = \frac{1}{(ab)^2} \int_{x_c}^{x_c+a} dx \int_{y_c}^{y_c+b} dy \int_0^a dx' \int_0^b dy' \frac{1}{\sqrt{(x-x')^2 + (y-y')^2 + h^2}} \tag{11}$$

There is an enlightening mathematical interpretation of the this equation. In free space, the static GF is just the inverse of the source-observer distance. Therefore, the quantity $1/\Psi$ (the inverse of our average discrete GF) can be viewed as the harmonic mean distance between two cells. And, correspondingly, $1/\Gamma$ is the harmonic mean distance between one cell and one point. So, Galerkin interactions between cells are equivalent to interactions between point charges separated by the harmonic mean distance between cells. Amazingly, this concept was familiar to Maxwell himself, who used it in a paper published in 1872 and entitled *"On the Geometrical Mean Distance of Two Figures on a Plane"* [13].

The 4D integral can be easily solved analytically, through the use of a smart change of variables which reduces the 4D-integral in (11) to a 2D-integral in the new variables $u = x - x'$ and $v = y - y'$, and leads to full analytical expressions for the MoM matrix elements (S1). The reduced 2D integral is:

$$c_{ij} = \frac{1}{(ab)^2} \int_{y-b}^{y+b} dv \int_{x-a}^{x+a} du \frac{\Lambda(u)\Lambda(v)}{\sqrt{u^2 + v^2 + h^2}} \tag{12}$$

where the triangular functions Λ are defined as:

$$\Lambda(u) = \begin{cases} u - x_c + a & ; \; x_c - a < u < x_c \\ x_c + a - u & ; \; x_c < u < x_c + a \end{cases} \quad ; \quad \Lambda(v) = \begin{cases} v - y_c + b & ; \; y_c - b < v < y_c \\ y_c + b - v & ; \; y_c < v < y_c + b \end{cases} \tag{13}$$

These triangular functions can be viewed as the cross-correlation or convolution of two pulse functions [14, sects.12-2 and 12-3]. In general, this change of variables transforms a 4D-integral involving a basis and a test function into a 2D-integral involving the correlation of these basis and test functions (S1). Similar devices have been previously used by other researchers. See for instance [15].

Inside the double integral (12) there are four different integrals, because the product of the triangular functions (13) will always result in a polynomial $Auv + Bu + Cv + D$.

The evaluation of (12) is then made by finding the 2D-primitives (indefinite double integrals) and invoking a generalized Fundamental Theorem of Calculus (S2).

The calculation of the 2D-primitives of these four integrals can be attempted using symbolic integration tools (Maple, Mathematica, MatLab, the open source Python Sympy...). But the results are sometimes disappointing and frequently hard to compare with classical results. Anyway, it would be a pity to renounce the pleasures of doing calculations by hand (a vanishing pre-computer wisdom) (S3). The four primitives needed are given in Table I.

Table I. *The 2D-primitives needed for eqn.12*

$f(u,v)$	$F(u,v) = \iint du\, dv\, f(u,v)$
$\frac{1}{\sqrt{u^2+v^2+h^2}}$	$u \sinh^{-1}\left(\frac{v}{\sqrt{u^2+h^2}}\right) + v \sinh^{-1}\left(\frac{u}{\sqrt{v^2+h^2}}\right) - h \tan^{-1}\left(\frac{uv}{h\sqrt{u^2+v^2+h^2}}\right)$

$\frac{u}{\sqrt{u^2+v^2+h^2}}$	$\frac{1}{2}[v\sqrt{u^2+v^2+h^2}+(u^2+h^2)\sinh^{-1}(\frac{v}{\sqrt{u^2+h^2}})]$
$\frac{v}{\sqrt{u^2+v^2+h^2}}$	$\frac{1}{2}[u\sqrt{u^2+v^2+h^2}+(v^2+h^2)\sinh^{-1}(\frac{u}{\sqrt{v^2+h^2}})]$
$\frac{uv}{\sqrt{u^2+v^2+h^2}}$	$\frac{1}{3}(u^2+v^2+h^2)^{3/2}$

Care must be exerted when evaluating some of these primitives in the particular case when h=0 and the variables u or v vanish. In practical implementations, a not very rigorous (but really practical) trick is always to avoid the coplanar situation by replacing the theoretical zero value of h for the smallest non zero value accepted by the computer language being used. Fortunately enough, this situation arises only when potentials are computed in the edges of the cells, which is not a usual need in MoM calculations.

These analytical formulas allow a complete analytical evaluation of our MoM matrix elements in (11). The first line in Table I is a generalization of a well-known expression, given by Wintle [16] for purely coplanar situations ($h=0$):

$$\int du\int dv\frac{1}{\sqrt{u^2+v^2}}=u\sinh^{-1}(v/|u|)+v\sinh^{-1}(u/|v|) \tag{14}$$

This is a very simple 2D-primitive; yet, it is hard to obtain it with symbolic software tools (S4).

With the use of these primitives, all the Galerkin MoM matrix elements can be analytically computed. This will allow us to solve practical problems involving single or parallel rectangular plates in the Galerkin framework. As a straightforward application, let us find the effect of a rectangular cell on itself (the diagonal terms in a Galerkin formulation). Here, we have $h=0$ and $x_c=y_c=0$. Then, by symmetry, (12) reduces to:

$$c_{ij}=\frac{4}{(ab)^2}\int_0^b dv\int_0^a du\frac{(u-a)(v-b)}{\sqrt{u^2+v^2}}=\frac{2}{b}\sinh^{-1}\frac{b}{a}+\frac{2}{a}\sinh^{-1}\frac{a}{b}+\frac{2}{3a^2b^2}[(a^3+b^3)-(a^2+b^2)^{3/2}] \tag{15}$$

This interesting result has been obtained by a direct application of (13) combined with the primitives of Table I. But for this particular case, the integral (15) is much easier and can be directly evaluated using polar coordinates. This provides a useful check of our work.

For the particular case of a unit square cell ($a=b=1$), we have the result:

$$c_{ii}=\int_0^1 dx\int_0^1 dy\int_0^1 dx'\int_0^1 dy'\frac{1}{\sqrt{(x-x')^2+(y-y')^2}}=4\sinh^{-1}(1)-\frac{4}{3}(\sqrt{2}-1)=2.9732 \tag{16}$$

This nice result has an interesting physical interpretation. In the self-case, Harrington's strategy of replacing cells by point charges located in their centers cannot be applied. But in a Galerkin strategy, the interaction between cells is equivalent to the interaction between point charges separated by the harmonic mean distance between cells. For the interaction of a unit square cell with itself (the MoM diagonal self-case), this distance is not zero. Rather, according to (16), it has a value $1/2.9732=0.3363$, practically one third of the cell's side.

If, instead of Galerkin, a Point-Matching strategy is used, we apply the Mean Value Theorem to (11) with the result:

$$c_{ij}=\Gamma(\mathbf{r_i},S_j)=\frac{1}{ab}\int_0^b dy'\int_0^a dx'\frac{1}{\sqrt{(x_c+a/2-x')^2+(y_c+b/2-y')^2+h^2}} \tag{17}$$

Again, the first line of Table I provides the complete solution of this integral. In this case, it could be more practical to define the origin of coordinates at the center of the source cell. Then, it becomes obvious that the above expression gives the normalized potential created at a point (x_c, y_c, h) by a rectangular cell of dimensions $a\times b$ located in the *xy* plane, centered at the origin and with unit total

This article has been accepted for publication in IEEE Antennas and Propagation Magazine. This is the author's version which has not been fully edited and content may change prior to final publication. Citation information: DOI 10.1109/MAP.2024.3362249

charge. For the particular case of a square cell ($a=b$) with unit total charge and points in its normal axis ($x_c=y_c=0$), we find the interesting result:

$$4\pi\varepsilon_0 V_{axis}(0,0,h)=\frac{4}{a}\sinh^{-1}\left(\frac{a}{\sqrt{a^2+4h^2}}\right)-\frac{4h}{a^2}\tan^{-1}\left(\frac{a^2}{2h\sqrt{2a^2+4h^2}}\right) \quad (18a)$$

Another special case of (17) is the PM self-case, with $x_c=y_c=0$ and $h=0$, which corresponds to the potential of a rectangular cell on its center:

$$c_{ii}=4\pi\varepsilon_0 V_{center}=\frac{2}{a}\sinh^{-1}(a/b)+\frac{2}{b}\sinh^{-1}(b/a) \quad (18b)$$

an expression which, in the particular case $a=b$ (square cell), fully agrees with the one given by Harrington [1, eqn.2.31], once the inverse hyperbolic sines are expressed as logarithms. In particular, for the unit square cell, we obtain the well-known numerical value $c_{ii}=3.5255$.

5. Implementation and test of the analytical expressions for Discrete and Averaged Discrete GFs

The analytical expressions for the Discrete GF, Γ_{ij} (eqn.17) and the Averaged Discrete GF Ψ_{ij} (eqn.11) have been implemented as the MatLab functions `DiscrGF` and `AvDiscrGF`, respectively (S5). Basis and test cells have the same dimensions $a\times b$ and the same orientation. For the implementation, it has been found handy to center the basis cell at the origin of coordinates. Then, the test cell center is at (x_c,y_c,z_c).

As a preliminary step, the analytical values of Γ_{ij} and Ψ_{ij} have been checked by making a rough direct numerical integration of the two-fold integral in (17) and the four-fold integral in (11) using standard quadratures. The results of these quadratures always converge towards the analytical values, although the convergence can be very slow and require a very large number of evaluation points if the basis and test cells are partially or totally overlapping. This is an additional proof for the validity of the analytical expressions, which are not only practically unavoidable for the self-case but can also save significant amounts of computer time in Galerkin approaches when cells are adjacent or close.

Once the analytical expressions of Discrete and Averaged Discrete Green's functions have been checked numerically, it is interesting to compare their values to foresee the possible differences that could be observed if different MoM approaches are applied to the same problem. For the comparison, we will consider unit square cells $(a=b=1)$.

Fig.3a provides, for a coplanar case with both cells in the $(z=0)$ plane, a graphical comparison between the three possible strategies, using Ψ, Γ and the plain Green's function approximation G. Here, the basis cell is centered at the origin and the test cell has its center on the *x*-axis, at $(x_c,0,0)$ with $0<x_c<2$. The functions Ψ,Γ and G (here given simply by $G=1/x_c$) are depicted, respectively, with blue, red and dashed black lines. While not evident in the plot, finer calculations with the same script show that the red line has an infinite derivative at $x_c=0.5$, which corresponds to the physical fact that the electric field is infinite at the edges of a charged plate. For distances roughly smaller than the cell half-size, Γ (PM) is greater than Ψ (Galerkin); but for larger distances, the Γ values remain systematically below Ψ. Then in fig. 3b, we explore, with the same color codes, the situation where the center of the test cell is located along the *z*-axis at $(0,0,z_c)$ with $0<z_c<2$. Here, Γ is always larger than Ψ and closer to GF values ($G=1/z_c$). The discrepancies in the self-case $(x_c=z_c=0)$ are quite significant, with Ψ being 18.6% smaller than Γ. But, for adjacent coplanar cells, Ψ is slightly larger than Γ (6.6%). As expected, the Galerkin dynamic range for the MoM matrix is lower than the PM range, since it involves an extra averaging over the test cell.

This article has been accepted for publication in IEEE Antennas and Propagation Magazine. This is the author's version which has not been fully edited and content may change prior to final publication. Citation information: DOI 10.1109/MAP.2024.3362249

The Green's approximation (not valid in the self-case) produces a large error in adjacent cells calculations (4% and 11% with respect to Γ and Ψ, respectively). But, as expected, both Γ and Ψ values converge quickly towards plain GF values, the differences between the three approaches being less than 0.5% when the distances between cells are larger than 5 times the cells' side.

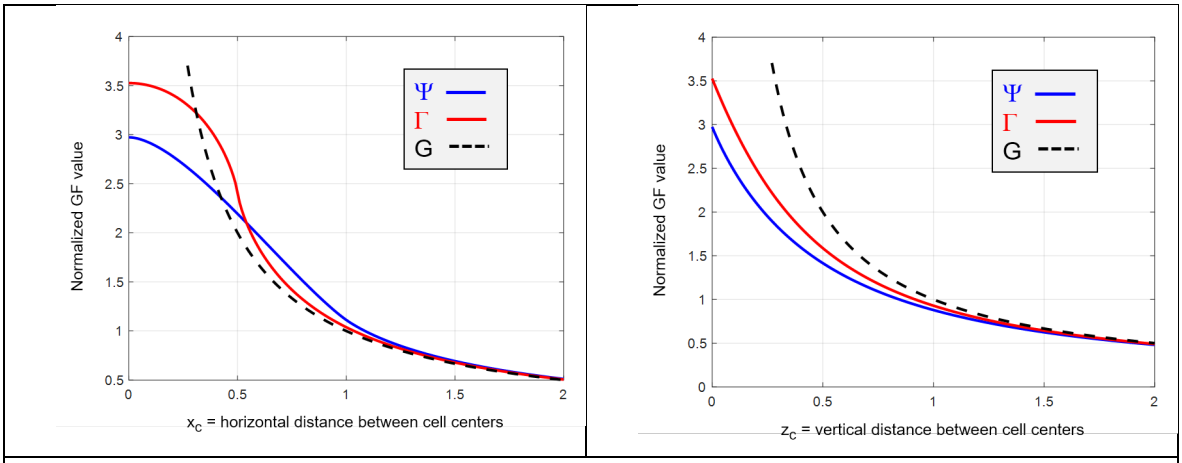

Fig.3: results for averaged discrete values (Galerkin, Ψ), discrete values (PM, Γ) and plain values (G) of the static free space Green's function. a) cells are centered on the *x*-axis (coplanar cells) b) cells are centered on the z-axis (parallel cells). Unit square cells are considered.

Therefore, it seems quite reasonable to replace Ψ or Γ values by approximated GFs when computing interactions between cells separated by a distance above a given threshold (say three or four times the cell's size). On the other hand, the bold Harrington strategy, replacing all PM values outside the main diagonal by GF values, seems a priori quite risky.

In any case, it is not mathematically easy to predict how a change in some elements of a linear system matrix will affect the values of the linear system solution (in our case, electric charge densities and capacitances). So, let us solve the problem and observe the results a posteriori.

6. Single plate at constant potential

We consider now the first electrostatic problem discussed by Harrington [1, sect. 2.2], the classic problem of a square unit metallic plate at a constant potential. Both the Galerkin and PM strategies have been implemented in a simple MatLab script `StaticPlate` (S5), able to deal with parallel rectangular plates divided into rectangular cells and optionally permitting the Harrington's simplification of using plain GF values as matrix elements. Because the analytical values of Γ_{ij} and Ψ_{ij} are used, no numerical integration routines are needed and the construction of the MoM matrix is simple and straightforward. For the excitation vector several classical options have been considered and the linear system is simply solved with the standard MatLab backslash "\" command. The solution vector contains the values of the total charges in every cell.

We consider first a single plate of dimensions $A \times B$ meters divided into $M \times N$ cells rectangular cells and at a fixed potential $4\pi\varepsilon_0 U = 1$. To reproduce Harrington's square plate, we select $A = B$ and $M = N$. Then, the total charge on the plate, which is the sum of all the cells' charges, gives directly the normalized capacitance C_{norm}. For a square plate of side A, the true capacitance in farads is $C = 4\pi\varepsilon_0 A C_{norm}$. Using the PM option, the MatLab script `StaticPlate` allow us to recover the charge values and the square plate capacitances given by Harrington in his book. But of course, we can now also try a Galerkin formulations and higher numbers of cells.

Fig.4 provides the results obtained for the normalized capacitance C_{norm} of a unit square plate $(A = 1)$ versus the number of cells N existing in the side of the plate, using both Point-Matching and Galerkin

This article has been accepted for publication in IEEE Antennas and Propagation Magazine. This is the author's version which has not been fully edited and content may change prior to final publication. Citation information: DOI 10.1109/MAP.2024.3362249

approaches. The two curves in black with crosses reproduce Harrington's results using his two PM strategies [1, Table 2.1]. Serendipity was at work here, because the "rough approx" scheme of Harrington (dashed black line) gave better results than his "exact" values (black continuous line).

For this problem, Harrington stopped his calculations with only 36 unknowns (N=6). We have reproduced his results and extended his curve up to 2500 unknowns (N =50) in the red curve with circles, where we can observe the typical slow convergence of PM. In the same figure, we have plotted the results obtained with a simplified Galerkin strategy (blue curve with squares). Results are better and exhibit a faster convergence. A Galerkin result with 400 unknowns is already much more accurate than a PM with 2500 unknowns. So, at least in some situations, it seems better to go for Galerkin and use a smaller number of unknowns, despite the increased analytical complexity.

Harrington's results were already good enough from an engineering point of view, his best point showing only a 3% error with respect to a converged Galerkin. And Harrington was able to extrapolate his results, asserting that *"a good estimate of the true capacitance is 40 picofarads"* [1, end section 2.2]. This corresponds to $C_{norm} = 0.360$ while our best Galerkin extrapolation is $C_{norm} = 0.3671$ ($C = 40.79$ pF/m), practically identical to the "best existing result" $C_{norm} = 0.3670$ (40.78 pF/m), published by B. Noble in 1971 [18], as duly acknowledged by Wintle [16] and reviewed by Kuester in his comprehensive survey paper [19] on microstrip patch capacitances.

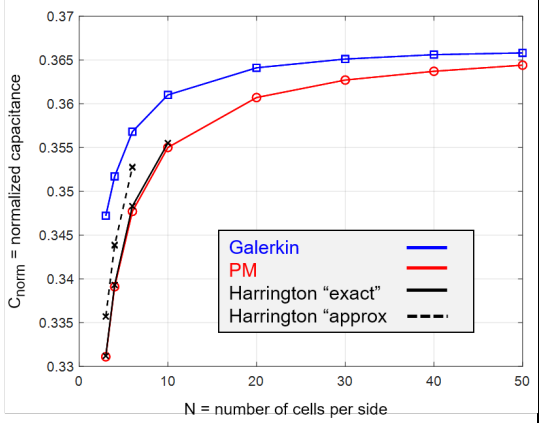

Fig.4 Normalized square plate capacitances for different MoM strategies as a function of the number *N* of cells per side (the total number of cells in the plate is N^2)

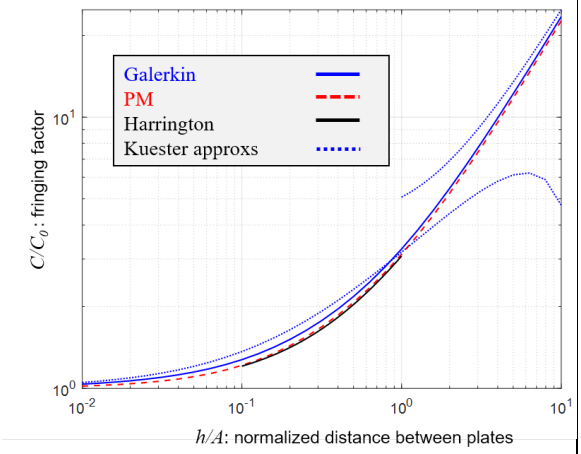

Fig. 5 The fringing factor C / C_0 of a square parallel plate capacitor as a function of the normalized distance between plates h/A.

Interestingly enough, in 1879 Maxwell himself had anticipated Harrington's strategy, using what we would call now a PM approach, when trying to provide a numerical justification to the empirical results of Cavendish for the capacitance of a square plate [20]. Maxwell cut the plate into 6x6 cells; hence the number of MoM unknowns would have been 36, but a clever use of symmetry reduced them to only 6 different unknowns. In an orthodox MoM approach, all the values of the diagonal elements c_{ii} must be identical if all the cells are identical. However, Maxwell's approach was rather unorthodox, because he slightly tweaked the results for the diagonal elements and made them dependent on the cell position (center, edge, corner) within the square plate. In addition, it seems that Maxwell made some numerical errors when solving his linear system of 6 unknowns by hand. Nevertheless, Maxwell was able to announce a value $C_{norm} = 0.361$ ($C = 40.1$ pF/m), within Cavendish experimental values ($C = 40.0 - 41.6$ pF/m) and perfectly aligned with modern results. This fascinating story has been studied in great detail by Wintle [16], who concluded his paper with a somewhat irreverent but justified remark: *"Evidently, Maxwell was not at the top of his form on this occasion".*

This article has been accepted for publication in IEEE Antennas and Propagation Magazine. This is the author's version which has not been fully edited and content may change prior to final publication. Citation information: DOI 10.1109/MAP.2024.3362249

7. The parallel plate condenser

As a second example, we consider the parallel plate condenser formed by two parallel square plates of side A separated by a distance h. This is a classic example treated by Harrington [1, sect.2.4] which became very relevant a few years later, when microstrip technology boomed in the early 1970s [21]. Harrington didn't make any use of symmetry between the two plates (this would be the correct approach when the plates are different). However, in a standard configuration the plates are identical and we can always assume them being at potentials $\pm V$ and exhibiting identical charges albeit of opposite sign $\pm Q$. Then, it is possible to still use here our script `StaticPlate`, modifying the GF as $G(\mathbf{r}\,|\,\mathbf{r}') = 1/|\mathbf{r}-\mathbf{r}'| - 1/|\mathbf{r}-\mathbf{r}'+h\hat{\mathbf{e}}_\mathbf{z}|$ and applying the MoM to just one plate. Once the total charge Q in the plate has been calculated, the capacitance is simply given by $C = |Q|/2V$. Following Harrington, we will concentrate on the calculation of the "fringing factor" C/C_0, where C is the MoM capacitance (thus including fringing fields) and C_0 is the classic parallel plate conductor formula, obtained by neglecting the fringing fields: $C_0 = \varepsilon_0 A^2/h$.

Fig. 5 gives the values of the fringing factor C/C_0 as a function of the normalized distance between plates h/A. Several approaches have been considered. The continuous blue curve gives the results obtained with a converged MoM implementation (N>10 in Galerkin or N>20 in PM) while the black curve reproduces as accurately as possible (S6) the results given by Harrington ([1], fig.2.7) for a shorter range of the distances between plates $0.1 < h/A < 1.0$.

The differences between these curves can be attributed to the insufficient discretization of the plate used and/or to some approximations used by Harrington [1, eqn. 2.43]. Indeed, if the PM version of our code is run with a lower number of cells (N=6) we obtain the dashed red curve which is practically on top of Harrington results and also agrees with Farrar&Adams [21]. Finally, the dotted blue curves correspond to the analytical asymptotic approximations for "small and large patches", given by Kuester in his complete study of microstrip patch capacitances [18, eqns 2.15 and 3.36]. Our numerical MoM results are perfectly framed by Kuester's asymptotic expressions.

A word of warning is needed here, because Harrington results [1, fig. 2.7] are slightly different in the three editions of his book (S6). Here, we have used the values extracted from the last 1993 edition, which seem the best or, at least, the ones closest to our PM results and to the numerical results obtained in 1972 by Farrar&Adams in their classic study of microstrip patches capacitances [21].

8. A single plate excited by a point charge

With minor modifications, the script `StaticPlate` can be used for many other interesting problems. For instance, to study the shielding effect of a metallic plate on the electric field created by a nearby point unit charge q placed at $\mathbf{r}_q$. In this case, the excitation vector components (9) are given by $e_i = -q/|\mathbf{r}_i - \mathbf{r}_q|$. We have selected a unit square plate in the $z=0$ plane with vertexes at (0,0,0), (1,0,0), (0,1,0), (1,1,0). A unit positive point charge is located above the plate center at (0.5,0.5,0.5). Our MatLab script using 20x20 cells and a PM strategy predicts a total induced charge in the plate $Q = -0.538$, which shows clearly that not all the field lines starting from the point charge are ending in the plate. The value obtained with Galerkin is less than 1% different. To check the validity of our calculations, we have plotted in one mid-plane of the plate $y=0.5$ the total potential due to the unit point charge and to the negative surface charge induced in the plate:

$$4\pi\varepsilon_0 V(\mathbf{r}) = \frac{q}{|\mathbf{r}-\mathbf{r_q}|} - \int_S ds' \frac{\rho_s(\mathbf{r}')}{|\mathbf{r}-\mathbf{r}'|} \approx \frac{q}{|\mathbf{r}-\mathbf{r_q}|} - \sum_{i=1,N} \frac{\alpha_i}{|\mathbf{r}_i-\mathbf{r_q}|} \qquad (19)$$

where the summation is to be extended to all the cells in the plate.

Fig.6 depicts the results obtained after adding the above equation to our MatLab script `StaticPlate`

and using the command `contourf` to visualize the equipotential lines. The deformation produced by the plate on these lines corresponds to the physics of the problem. Some lines still enclose the point charge, while trying to go around the plate. Other lines do not enclose the point charge any longer but the plate; and the equipotential zero becomes the plate itself. Also, the concentration of the lines just above the plate tell us about strong field values there.

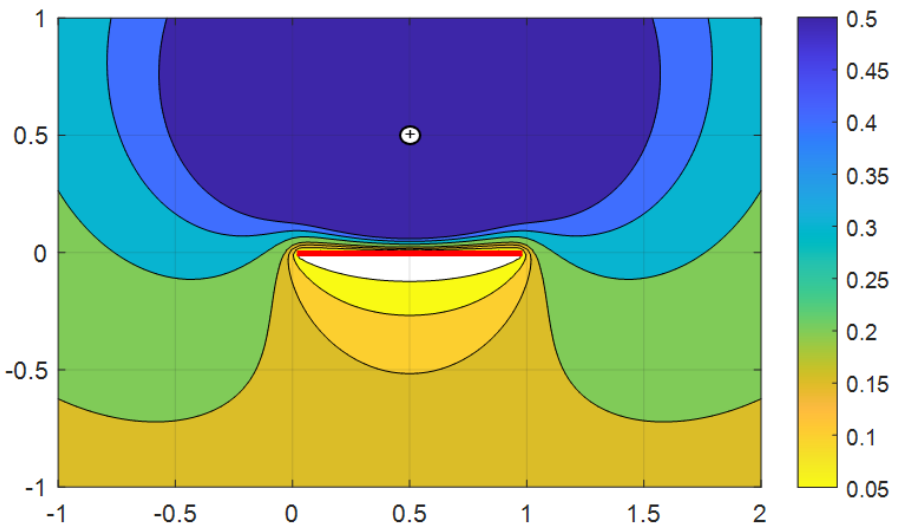

Fig.6 Equipotential lines in the median plane of a square plate excited by a point charge above its center

9. Three-dimensional plots

In the 1960's, 3D plots were only a researcher's dream; no wonder that they cannot be found in Harrington's book. Today however, they are routinely offered by popular software tools like MatLab.

Figure 7 contains several 3D plots of the normalized surface charge density, obviously obtained by dividing the total charge in every cell (the unknowns in our MoM implementation `StaticPlate`) by the cell's surface areas. A relatively modest grid of 20x20 cells has been used.

Figs 7a and 7b refer to the single plate of section 6. Two drawing strategies have been used. In Fig. 7a, the values of the piecewise constant basis functions in every cell have been depicted as realistically as possible. In Fig. 7b we have just plotted the same numerical values using the MatLab command `surf`. Observing these two graphs, one wonders whether the interpolation scheme in the plotting routine `surf` is producing a result equivalent to the one we could have obtained using higher order basis functions, like piecewise linear ones.

In Fig. 7c the charge density is that existing in the upper plate of a parallel plate condenser with $A = 1$ and $h / A = 0.1$ (section 7). It is interesting to compare the graph with that in Fig.7a, corresponding to a single plate $(h \to \infty)$. Of course, here a quantitative comparison is meaningless. But the change in the shape of the charge density is remarkable, the two close plates of a parallel condenser resulting in a much more uniform distribution, save for the well-known edge fringing effects. Finally, Fig. 7d is a `surf` plot of the absolute value of the negative charge density appearing in the problem of section 8. The effect of the point charge is clearly apparent as a "bulge" in the center of the plate and a slight distortion of the charge profile in the edges of the plate.

All the results used to generate the fig.7 were obtained using a PM approach. But no differences visible to the naked eye would appear if a Galerkin strategy were used. A closer comparison, using 50x50 cells and singling out the values of the charge in the median line of the plate (as done in [1], fig. 2.2), reveals that the differences between the surface charge density values obtained by using PM and Galerkin strategies remain below 1%, except for the cells closer to the edges where differences of up to 7% can be observed. These differences near edges and corners are not surprising at all. Charge distributions with singularities cannot be exactly simulated with bounded basis functions. Fortunately enough, the integration (here sum) of the cells' charge values is an error-cancelling process and simple

This article has been accepted for publication in IEEE Antennas and Propagation Magazine. This is the author's version which has not been fully edited and content may change prior to final publication. Citation information: DOI 10.1109/MAP.2024.3362249

pulse basis functions are enough to obtain remarkably accurate results for the capacitance values. While we should always expect Galerkin to perform better than PM when approaching a regular continuous function, this is not the granted in problems involving singular surface charge distributions. Of course, it is always possible to select higher-order basis functions, possibly including singular behaviors. This is still an ongoing hot topic, as can be seen in recent works [22-23]. Systematic convergence studies and detailed comparisons of different possible basis/test functions choices are outside the scope of this paper and have been treated in several authoritative books [5, 24-25].

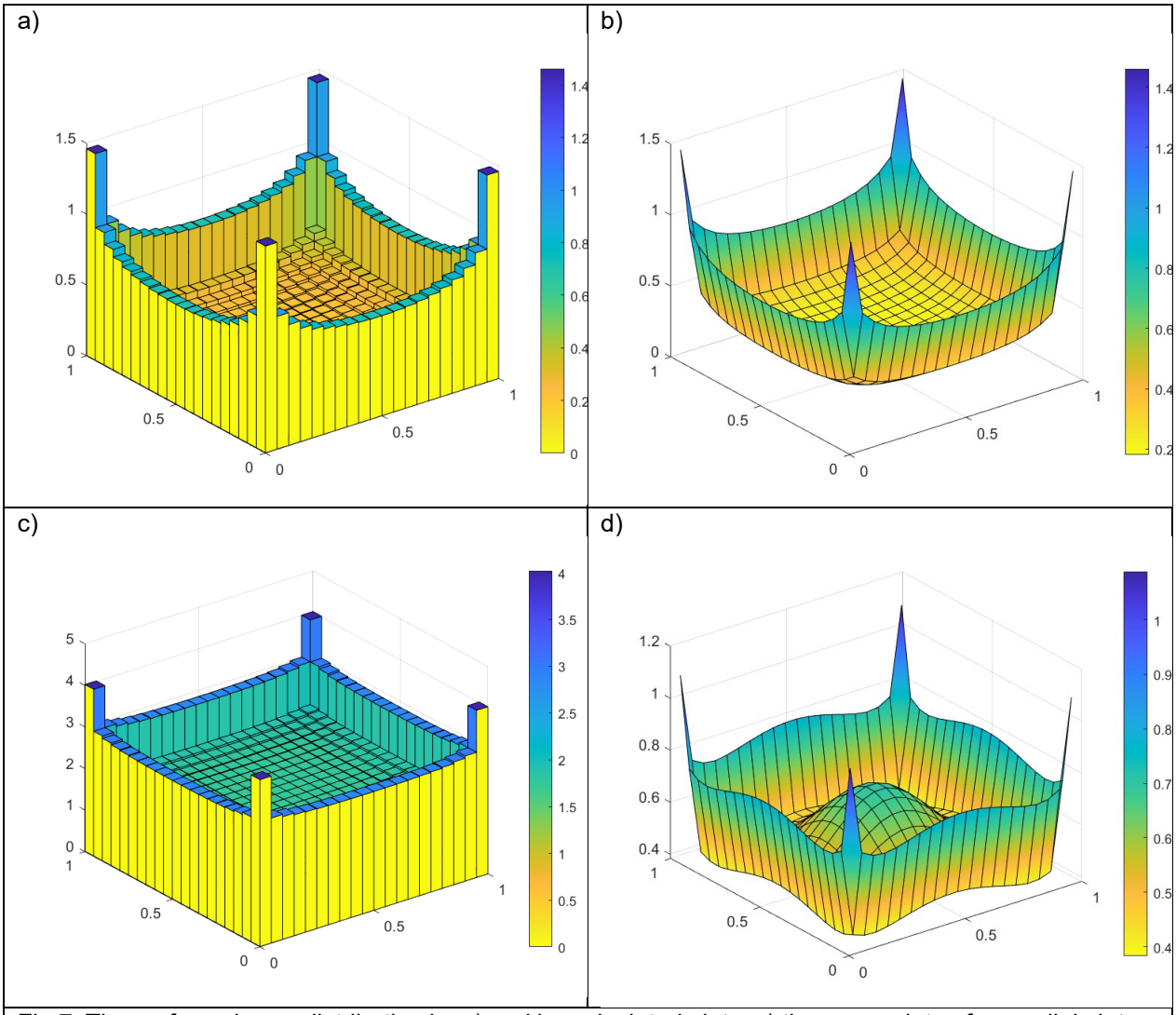

Fig.7. The surface charge distribution in: a) and b: an isolated plate; c) the upper plate of a parallel plate condenser with h/A =0.1 ; d) a plate excited by a point charge above it and on its normal axis

10. Concluding remarks

In this first part of the paper, we have concentrated on revisiting some electrostatics examples included by Roger F. Harrington in his epoch-making book "Field Computation by Moment Methods". While checking his pioneering results and highlighting their excellent quality, we have generalized them into a fully analytical formulation, which provides a systematic treatment and illuminating insights for configurations not previously treated. Our study has also allowed us to unearth some interesting historical facts which are barely known nowadays. It might be considered superfluous to treat in such a detail a series of purely electrostatic situations, especially in an Antennas&Propagation publication. But this would be short-sighted. As discovered by Harrington himself, when time-harmonic full wave problems are formulated in the context of a Mixed Potential Integral Equation (MPIE), the mathematical

parallelisms with the static Potential Integral Equation (PIE) make all the electrostatic formulations developed here not only useful but also unavoidable when dealing with electrodynamic problems. Indeed, a reasonably accurate free-space MPIE software tool can be built by using the static discrete Green's functions developed here. In fact, the only additional complexity is that we will be dealing with a vectorial unknown (the electrodynamic surface current density) rather than with a scalar one (the electrostatic surface charge density). This will be clearly demonstrated in the second part of this paper.

Acknowledgements

Thanks are given to Dr. P. Crespo-Valero, Prof. G. Eleftheriades, Dr. R. C. Hall, Prof. E.F. Kuester and Dr. I. Stevanovic for their invaluable help in preparing this manuscript.

References

[1] R. F. Harrington, “Field Computation by Moment Methods”; 1st edition Macmillan, New York 1968; 2nd edition Krieger, Malabar, FL,1982; 3rd edition IEEE Press Series on Electromagnetic Wave Theory, 1993.
[2] R. F. Harrington, "Origin and development of the method of moments for field computation," in IEEE Antennas and Propagation Magazine, vol. 32, no. 3, pp. 31-35, June 1990 (reprinted in [4]).
[3] L. Kantorovich and G. Akilov, Functional Analysis in Normed Spaces,D. E. Brown, trans. Oxford: Pergamon, 1964, pp. 586-587.
[4] E. K. Miller, L. Medgyesi-Mitschang and E. H. Newman eds., “Computational Electromagnetics: Frequency-Domain MoM”, IEEE Press, Piscataway, NJ, 1992
[5] W. C. Gibson, " The Method of Moments in Electromagnetics", 3rd Edition, Chapman & Hall, 2021
[6] R. F. Harrington, “Time-Harmonic Electromagnetic Fields”, 1961. Reissued, IEEE Press Series on Electromagnetic Wave Theory, 2001.
[7] D. R. Wilton, "History of developments leading to the method of moments," 2018 International Applied Computational Electromagnetics Society Symposium (ACES), 2018, pp. 1-2
[8] R. F. Harrington, "Matrix methods for field problems", Proceedings of the IEEE, vol. 55, no. 2, pp. 136-149, Feb. 1967
[9] J. C. Rautio, "Roger Harrington and shielded planar microwave electromagnetic analysis," 2018 International Applied Computational Electromagnetics Society Symposium (ACES), 2018, pp. 1-2
[10] A. R. Djordjević and T. K. Sarkar, “A theorem on the moment methods”, Trans. IEEE, vol. AP-35, no. 3, March 1987, pp.353-355..
[11] S. Lopez-Pena, J. R. Mosig, Analytical evaluation of the quadruple static potential integrals on rectangular domains to solve 3-d electromagnetic problems, IEEE Transactions on Magnetics 45 (3) (2009) 1320–1323.
[12] M. De Lauretis, E. Haller, F. Di Murro, D. Romano, G. Antonini, J. Ekman , I. Kovacevic-Badstübner, U. Grossner, " On the rectangular mesh and the decomposition of a Green’s-function-based quadruple integral into elementary integrals" Engineering Analysis with Boundary Elements 134, pp. 419–434, 2022
[13] J. Clerk Maxwell, "On the Geometrical Mean Distance of Two Figures on a Plane", Transactions of the Royal Society of Edinburgh, vol. XXVI, part. IV, 1872, pp.729-733
[14] A. Papoulis, "The Fourier Integral and its Applications, McGraw-Hill, New York, 1962.
[15] T. F. Eibert and V. Hansen, “On the calculation of potential integrals for linear source distributions on triangular domains,” IEEE Trans. Antennas Propag., vol. 43, no. 12, pp. 1499–1502, Dec. 1995.
[16] H. J. Wintle, "Maxwell and the boundary element method: a historical puzzle," in IEEE Electrical Insulation Magazine, vol. 14, no. 6, pp. 23-25, Nov.-Dec. 1998
[17] J. H. Wilkinson, "Rounding Errors in Algebraic Processes" (Prentice-Hall Series in Automatic Computation), Prentice-Hall, Inc., NY, 1963
[18] B. Noble, "Some Applications of the Numerical Solution of Integral Equations to Boundary Value Problems," in Conference on Applications of Numerical Analysis, ed. J. LL Morris, Springer, Berlin, 1971, pp. 137-154.
[19] E.F. Kuester "Explicit Approximations for the Static Capacitance of a Microstrip Patch of Arbitrary Shape", Journal of Electromagnetic Waves and Applications, 2:1, 103-135, 1988
[20] 5. J. Clerk Maxwell, ed., Electrical Researches of the Honourable Henry Cavendish, FRS, University Press, Cambridge, 1879, pp. 426-427 https://archive.org/details/electricalresear00caveuoft/page/426
[21] A. Farrar and A. T. Adams, "Matrix Methods for Microstrip Three-Dimensional Problems," *IEEE Transactions on Microwave Theory and Techniques,* vol. 20, no. 8, pp. 497-504, Aug. 1972
[22] A. F. Peterson and R. D. Graglia, "Relative Impact of Singular Edge and Corner Basis Functions on the Capacitance of Parallel-plate Capacitors," 2021 International Conference on Electromagnetics in Advanced Applications (ICEAA), Honolulu, HI, USA, 2021, pp. 414-415
[23] R. D. Graglia, A. F. Peterson and P. Petrini, "Hierarchical Divergence Conforming Bases for Tip Singularities in Quadrilateral Cells," in IEEE Transactions on Antennas and Propagation, vol. 68, no. 12, pp. 7986-7994, Dec. 2020
[24] R. Mittra and C.A. Klein, "Stability and convergence of moment method solutions", in Numerical and Asymptotic Techniques in Electromagnetics, ed. R. Mittra, Springer, New York, 1975
[25] A. F. Peterson, S. L. Ray, R. Mittra, "Computational Methods for Electromagnetics", Wiley-IEEE Press, 1997.

SUPPLEMENTARY MATERIAL FOR:
"Roger F. Harrington and the Method of Moments; Part 1: Electrostatics"

Juan R. Mosig, IEEE AP Magazine, 2024

S1. A "correlation" strategy to reduce 4D integrals involving GFs to 2D-integrals.

The Galerkin interaction between two rectangular cells situated in parallel planes and having identical orientations can be advantageously solved with a change of variables which is related to the convolution and cross-correlation operations used in signal processing. The basic idea is to reorder the four integrals in equation (11), giving the MoM Galerkin elements, as:

$$c_{ij} = \Psi(S_i, S_j) = \frac{1}{(ab)^2} \int_{y_c}^{y_c+b} dy \int_0^b dy' \int_{x_c}^{x_c+a} dx \int_0^a dx' \frac{1}{\sqrt{(x-x')^2+(y-y')^2+h^2}}$$

and apply successively the same strategy to the couple of integrals on *x/x′* and on *y/y′*.

Let us consider the inner *x/x′* double integral, but in a generalized version, where the subsectional basis and test functions are not necessarily pulse functions and the involved GF is not necessarily the free space one:

$$I = \int_{x_c}^{x_c+a} dx\, t(x) \int_0^a dx'\, b(x') G(x-x')$$

Then we apply the change of variables $u = x - x'$ and $p = x'$. The Jacobian of the transformation has unit value, so we have $dx\,dx' = dp\,du$. According to the geometrical depiction visualizing the new axis *u* (figure)

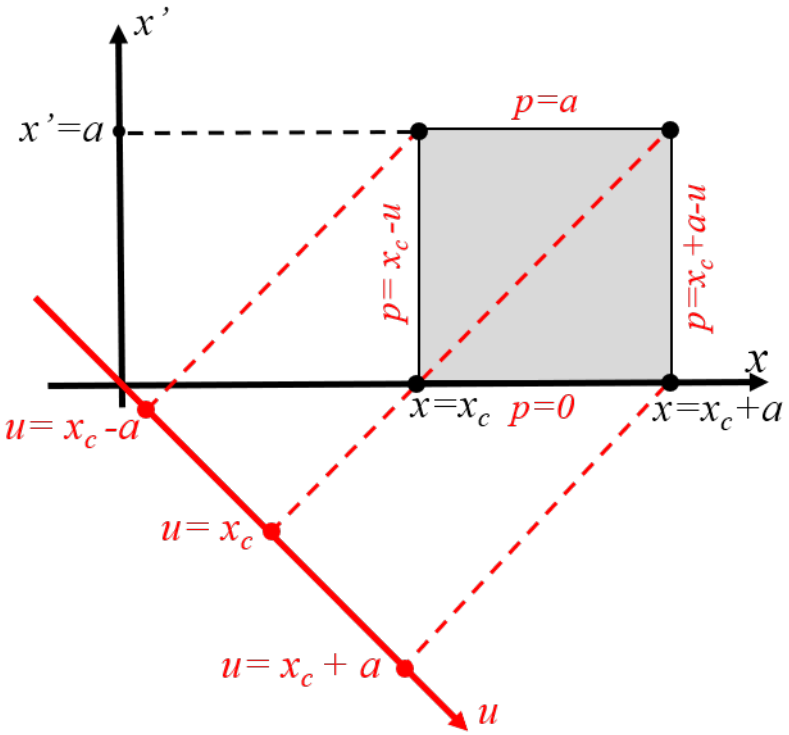

the bounds of the *x/x′* domain, given by $(x = x_c \;;\; x = x_c + a \;;\; x' = 0 \;;\; x' = a)$, become $(p = x_c - u \;;\; p = x_c + a - u \;;\; p = 0 \;;\; p = a)$ and the integral can be rewritten as:

$$I=\int_{x_c-a}^{x_c} du\, G(u) \int_{p=x_c-u}^{p=a} dp\, b(p) t(u+p) + \int_{x_c}^{x_c+a} du\, G(u) \int_{p=0}^{p=x_c+a-u} dp\, b(p) t(u+p)$$

or in a more compact form as: $I=\int_{x_c-a}^{x_c+a} du\, G(u) C(u)$

with the function *C(u)* being given by:

$$C(u)=\begin{cases} \int_{p=x_c-u}^{p=a} dp\, b(p) t(u+p) & \text{for} \quad x_c-a<u<x_c \\ \int_{p=0}^{p=x_c+a-u} dp\, b(p) t(u+p) & \text{for} \quad x_c<u<x_c+a \end{cases}$$

and being zero elsewhere.

For many subsectional basis functions (piecewise constant, piecewise linear...) the function *C(u)* has a simple analytical expression. For instance, for piecewise constant functions (pulses), as studied in the paper, we simply have:

$$C(u)=\begin{cases} u-(x_c-a) & \text{for} \quad x_c-a<u<x_c \\ (x_c+a)-u & \text{for} \quad x_c<u<x_c+a \end{cases}$$

If now the whole procedure is repeated with the outer y/y' double integral, and the free-space GF is used, we immediately arrive to equations (12-13) in the paper.

It is worth mentioning that due to the subsectional character of our basis and test functions (being non-zero only in finite bounded domains), the integration limits in the integrals defining *C(u)* can be extended to infinity and we can write for *C(u)* a single formula:

$$C(u)=\int_{-\infty}^{+\infty} dp\, b(p) t(u+p) \quad \text{for} \quad -\infty<u<+\infty$$

Hence, *C(u)* is the cross-correlation between the basis and test functions; and it is simply the auto-correlation of the basis function if a Galerkin approach is considered. See Papoulis [14, sects.12-2 and 12-3].

The above described change of variables has been independently developed by this author. But the subjacent idea is a very logical one and the same device (or very similar ones) has been used in related MoM problems by many authors, to reduce 4D integrals to 2D ones. A pioneer work, albeit limited to the self-case, that should be mentioned is the reference [15] in the paper.

S2. A pedestrian generalization of the Fundamental Theorem of Calculus.

Consider the definite integral $I=\int_{x_1}^{x_2} dx\, f(x)$. Then, if there is a function $F(x)$ (called primitive or antiderivative of $f(x)$) satisfying the relationship: $f(x)=\frac{d}{dx}F(x)$, we can assert that:

$$I=\int_{x_1}^{x_2} dx\, f(x)=F(x_2)-F(x_1)$$

This is the Fundamental Theorem of Calculus. Its generalization to multiple dimensions is not an easier subject and can only be found in books specialized on multivariable calculus. In two dimensions, and

for arbitrarily shaped integration domains, the generalization is done via the theorems of Stokes, Green and related ones. Moreover, it is frequently stated that *"since the concept of an antiderivative is only defined for functions of a single real variable, the usual definition of the indefinite integral does not immediately extend to the multiple integral"* (https://en.wikipedia.org/wiki/Multiple_integral).
However, if the integration domain is a rectangle with sides parallel to the coordinate axes, then the integration limits are constant values and the double integral can be viewed as a repeated or iterated integral. In this case the obvious extension to two dimensions is:

$$I=\int_{y_1}^{y_2} dy \int_{x_1}^{x_2} dx\, f(x,y) = F(x_2,y_2)-F(x_1,y_2)-F(x_2,y_1)+F(x_1,y_1) = \sum_{i=1,2}\sum_{j=1,2}(-1)^{i+j}F(x_i,y_j)$$

where the function F must fulfill the condition $\dfrac{\partial^2}{\partial x\,\partial y}F(x,y)=f(x,y)$.

In the one-dimensional case, the primitive is defined "up to a constant". In other words, if $F(x)$ is a primitive, also is $F(x)+C$. The extension to two dimensions is obvious: if $F(x,y)$ is a primitive, also is $F(x,y)+X(x)+Y(y)+C$, where $X(x)$ and $Y(y)$ are arbitrary functions of a single variable.
This fact can sometimes be used to simplify the expressions of some 2D-primitives.
The generalization to hyperrectangles in higher dimensions is easily made. For instance, for four dimensions:

$$I=\int_{v_1}^{v_2} dv\int_{u_1}^{u_2} dy\int_{y_1}^{y_2} dy\int_{x_1}^{x_2} dx\, f(x,y) = \sum_{m=1,2}\sum_{n=1,2}\sum_{i=1,2}\sum_{j=1,2}(-1)^{m+n+i+j}F(x_i,y_j,u_m,v_n)$$

where F is any possible primitive function satisfying the condition: $\dfrac{\partial^4}{\partial x\,\partial y\,\partial u\,\partial v}F(x,y,u,v)=f(x,y,u,v)$

With these definitions in mind, the numerical quadrature of multidimensional definite integrals can be advantageously replaced by the evaluation of the adequate multidimensional primitives, if analytically available.

S3. The 2D-primitives of Table I (a lot of fun!)

Here, the integration is along the coordinates *u,v*. The third coordinate has a constant value $z=h$.

I) 2D-primitive of $f(u,v)=\dfrac{1}{\sqrt{u^2+v^2+h^2}}$.

This primitive can find using elementary integration techniques.

First, we integrate along u: $P_u=\int\dfrac{du}{\sqrt{u^2+v^2+h^2}}=\sinh^{-1}\left(\dfrac{u}{\sqrt{v^2+h^2}}\right)$

And then we must find $F(u,v,h)=\int dv\, P_u=\int dv\,\sinh^{-1}\left(\dfrac{u}{\sqrt{v^2+h^2}}\right)$

This integral can be solved by integration by parts:

$$F(u,v,h)=v\sinh^{-1}\left(\frac{u}{\sqrt{v^2+h^2}}\right)+u\int dv\,\left(1-\frac{h^2}{v^2+h^2}\right)\left(\frac{u}{\sqrt{u^2+v^2+h^2}}\right)=v\sinh^{-1}\left(\frac{u}{\sqrt{v^2+h^2}}\right)+u(I_1-h^2I_2)$$

for the first auxiliary integral I_1 , the result is straightforward $I_1 = \frac{dv}{\sqrt{v^2+u^2+h^2}} = \sinh^{-1}(\frac{v}{\sqrt{u^2+h^2}})$

.

The second auxiliary integral I_2 can be found in the tables (Gradshteyn 2.282.2 and 2.281) (or if you are younger, using a symbolic software like Mathematica or Maple):

$$I_2 = \int dv\,(\frac{1}{v^2+h^2})(\frac{1}{\sqrt{u^2+v^2+h^2}}) = \frac{1}{uh}\tan^{-1}\frac{uv}{h\sqrt{u^2+v^2+h^2}}$$

So finally our 2D-primitive is (first line in Table I):

$$F(u,v,h) = \int dv \int du \frac{1}{\sqrt{u^2+v^2+h^2}} = u\sinh^{-1}(\frac{v}{\sqrt{u^2+h^2}}) + v\sinh^{-1}(\frac{u}{\sqrt{v^2+h^2}}) - h\tan^{-1}\frac{uv}{h\sqrt{u^2+v^2+h^2}}$$

The case $h=0$ is of interest for purely coplanar problems. We get:

$$F(u,v,0) = \int dv \int du \frac{1}{\sqrt{u^2+v^2}} = v\sinh^{-1}\left(\frac{u}{|v|}\right) + u\sinh^{-1}\left(\frac{v}{|u|}\right)$$

a classical result by obtained by Wintle (eqn. 14 in the paper).

II) 2D-primitive of $f(u,v) = \frac{u}{\sqrt{u^2+v^2+h^2}}$. This primitive will provide the second and third lines in Table I. The integration along *u* is easy and immediate:

$$P_u = \int \frac{udu}{\sqrt{u^2+v^2+h^2}} = \sqrt{u^2+v^2+h^2}$$

Now we need $F(u,v,h) = \int dv \sqrt{u^2+v^2+h^2}$ and the result is (Gradshteyn 2.271.3):

$$F(u,v,h) = \int dv \int du \frac{u}{\sqrt{u^2+v^2+h^2}} = \frac{1}{2}[v\sqrt{u^2+v^2+h^2} + (u^2+h^2)\sinh^{-1}(\frac{v}{\sqrt{u^2+h^2}})]$$

which reduces in the particular case $h=0$ to: $F(u,v,0) = \frac{1}{2}[v\sqrt{u^2+v^2} + u^2\sinh^{-1}(\frac{v}{|u|})]$

III) Finally, we need the 2D-primitive of $f(u,v) = \frac{uv}{\sqrt{u^2+v^2+h^2}}$

This is the easiest one, with $P_u = \int \frac{uvdu}{\sqrt{u^2+v^2+h^2}} = v\sqrt{u^2+v^2+h^2}$

and: $F(u,v,h) = \int dv\, v\sqrt{u^2+v^2+h^2} = \frac{1}{3}(u^2+v^2+h^2)^{3/2}$

In the particular case $h=0$, it reduces to: $F(u,v,0) = \frac{1}{3}(u^2+v^2)^{3/2}$

The Table I in the paper, combined with the 2D-generalization of the Fundamental Theorem of Calculus, allows us to obtain many interesting results like those in eqns (15,16,18) of the paper. Its first line can be used to compute the analytical expression of the normalized electrostatic potential created in a generic point (x,y,h) by a rectangular cell of dimensions $a\times b$ located in the *xy* plane,

centered at the origin and with total unit charge. For instance, for a square cell of unit side, we have these results:

- at its center: $4\pi\varepsilon_0 V = 4F(0.5,0.5,0) = 4\sinh^{-1}(1) = 3.5255$,

- in an edge's mid-point: $4\pi\varepsilon_0 V = 2F(1,0.5,0) = 2\sinh^{-1}(1/2) + \sinh^{-1}(2)/2 = 2.4061$

- in a corner: $4\pi\varepsilon_0 V = F(1,1,0) = 2\sinh^{-1}(1) = 1.7627$ (obviously, half of the value at the center)

- and at a height 0.5 above the center: $4\pi\varepsilon_0 V = 4F(0.5,0.5,0.5) = 4\sinh^{-1}\left(\sqrt{2}/2\right) - \pi/3 = 1.5867$

Even more interesting, analytic differentiation of the potential yields all the components of electric field created by such a rectangular cell and allows the study of the singularities arising in special points like corners and edges. This exciting development is left to the reader.

S4. 2D-primitives with symbolic software tools

It is interesting to check whether all these primitives can be also found through the use of symbolic software tools. Their computational power increases year after year and version after version and the future clearly belongs to them. Yet, in its current state, their results can be surprising and require a lot of post-processing to make them appear in a compact and elegant form.

For instance, the author has tried to compute the first 2D-primitive of the previous section with the Online Integral Calculator from WolframAlpha, freely available in the Internet: https://www.wolframalpha.com/calculators/integral-calculator/?src=google&388=free software (accessed on July 24, 2023). The somewhat awkward result was obtained:

https://www.wolframalpha.com/input?i2d=true&i=Integrate%5BDivide%5Bx%2CSqrt%5BSquare%5Bx%5D%2BSquare%5By%5D%2BPower%5Bh%2C2%5D%5D%5D%2Cx%2Cy%5D

Input

$$\int\int \frac{1}{\sqrt{x^2+y^2+h^2}}\,dy\,dx$$

Result

$$\frac{1}{2}\left(-x\log\left(1-\frac{y}{\sqrt{h^2+x^2+y^2}}\right)+x\log\left(\frac{y}{\sqrt{h^2+x^2+y^2}}+1\right)+2\,y\log\left(\sqrt{h^2+x^2+y^2}+x\right)-2\,h\tan^{-1}\left(\frac{x\,y}{h\sqrt{h^2+x^2+y^2}}\right)\right)$$

Indefinite integral

$$\int\int \frac{1}{\sqrt{x^2+y^2+h^2}}\,dy\,dx = c_1\,y+c_2-\frac{1}{2}\,y\log\left(1-\frac{x}{\sqrt{h^2+x^2+y^2}}\right)+\frac{1}{2}\,y\log\left(\frac{x}{\sqrt{h^2+x^2+y^2}}+1\right)+x\log\left(\sqrt{h^2+x^2+y^2}+y\right)-h\tan^{-1}\left(\frac{x\,y}{h\sqrt{h^2+x^2+y^2}}\right)$$

$\tan^{-1}(x)$ is the inverse tangent function

$\log(x)$ is the natural logarithm

Hopefully the two seemingly different expressions labelled "Result" and "Indefinite integral" (where the expected x-y symmetry is not readily evident) are both equivalent to our result (first line in Table I of the paper). But the demonstration will certainly require some tricky playing (left to the reader) with the logarithms to arrive to the compact and elegant expression obtained with the inverse hyperbolic sinus

Then, if a numerical value of h is tried, for instance $h=1$, the Online Integral Calculator provides this very surprising result, including imaginary logarithms:

https://www.wolframalpha.com/input?i2d=true&i=Integrate%5BDivide%5B1%2CSqrt%5BSquare%5Bx%5D%2BSquare%5By%5D%2B1%5D%5D%2Cx%2Cy%5D

Input

$$\int\int \frac{1}{\sqrt{x^2+y^2+1}}\,dy\,dx$$

Result

$$\frac{1}{4}\left(-2x\log\left(1-\frac{y}{\sqrt{x^2+y^2+1}}\right)+2x\log\left(\frac{y}{\sqrt{x^2+y^2+1}}+1\right)+4y\log\left(\sqrt{x^2+y^2+1}+x\right)-i\log\left(\frac{4i\left(y\sqrt{x^2+y^2+1}+ix+y^2+1\right)}{(x-i)y^2}\right)-i\log\left(\frac{4\left(x-i\left(y\sqrt{x^2+y^2+1}+y^2+1\right)\right)}{(x-i)y^2}\right)+i\log\left(-\frac{4\left(x+i\left(y\sqrt{x^2+y^2+1}+y^2+1\right)\right)}{(x+i)y^2}\right)+i\log\left(\frac{4\left(x+i\left(y\sqrt{x^2+y^2+1}+y^2+1\right)\right)}{(x+i)y^2}\right)\right)$$

$\log(x)$ is the natural logarithm

Indefinite integral

$$\int\int \frac{1}{\sqrt{x^2+y^2+1}}\,dy\,dx = \frac{1}{4}\left(4c_1y+4c_2-2y\log\left(1-\frac{x}{\sqrt{x^2+y^2+1}}\right)+2y\log\left(\frac{x}{\sqrt{x^2+y^2+1}}+1\right)+4x\log\left(\sqrt{x^2+y^2+1}+y\right)-i\log\left(\frac{-ix\sqrt{x^2+y^2+1}-ix^2+y-i}{x^2(y-i)}\right)+i\log\left(\frac{ix\sqrt{x^2+y^2+1}+ix^2+y+i}{x^2(y+i)}\right)+i\log\left(\frac{x\sqrt{x^2+y^2+1}+x^2-iy+1}{x^2(-1+iy)}\right)-i\log\left(\frac{x\sqrt{x^2+y^2+1}+x^2+iy+1}{x^2(-1-iy)}\right)\right)$$

$\log(x)$ is the natural logarithm

S5. The MatLab scripts

The first script `definite` implements simply our generalized theorem of calculus for 2D integrals:

```
function [value] = definite(prim,x1,x2,y1,y2)
% "definite" is just the combination of four values of the 2D-primitive
% "prim" of a function f(x,y).
% Therefore, it gives the value of the double integral of f(x,y)
% over the rectangular domain (x1,x2,y1,y2)
value=prim(x1,y1)+prim(x2,y2)-prim(x1,y2)-prim(x2,y1);
end
```

The analytical expressions for the Discrete GF, Γ_{ij} (eqn.17) and the Averaged Discrete GF Ψ_{ij} (eqn.11) have been implemented as the MatLab functions `DiscrGF` and `AvDiscrGF`, respectively. `AvDiscrGF` calls the script `definite`.

Basis and test cells have the same dimensions $a \times b$ and the same orientation. The basis cell is always centered at the origin of coordinates and the test cell center is at (x_c, y_c, z_c).

```
% DiscrGF computes a free space Discrete Green's function associated
% to the scalar potential potential created in the point (xc,yc,zc)
% by a rectangular cell of dimensions a*b, centered at the origin
% and located in the plane xy, with sides parallel to the x and y axes
% The computation is done by evaluating the normalized surface integral
% (giving the mean value of the integrand 1/r, through the use of
% the primitive function prim1

% DiscrGF is to be used in Point-Matching formulations. If the Mean Theorem
%is used, DiscrGF can be approximated by the corresponding GF value (=1/r)

% To avoid 0/0 indeterminacies the value zc is replaced by zc+eps with
% eps=2.2204e-16. This has in negligeable effect in the obtained values
% A total unit charge is assumed in the cell. Hence, the electrostatic
% potential is obtained multiplying the result by the factor:
% (total cell charge)/(4*pi*eps0)

% J. R. Mosig, EPFL Switzerland, 01/06/2023

function [result] = DiscrGF(xc,yc,zc,a,b)

   prim1 = @(u,v,c) u*asinh(v/sqrt(u^2+c^2))+v*asinh(u/sqrt(v^2+c^2))...
      -c*atan(u*v/c/sqrt(u^2+v^2+c^2));
   zc=zc+eps;
   result=prim1(xc+a/2,yc+b/2,zc)+prim1(xc-a/2,yc-b/2,zc)...
         -prim1(xc+a/2,yc-b/2,zc)-prim1(xc-a/2,yc+b/2,zc);
   result=result/(a*b);
end
```

```
% AvDiscrGF computes a free space Averaged Discrete Green's function
% giving the electrostatic interaction between two rectangular cells of
% identical dimensions a*b and located in the planes z=0 and z=zc, both
% having sides parallel to the x and y axes.
% The centers of the two cells are in (0,0,0) and (xc,yc,zc).

% The computation is done by evaluating the normalized double surface (4D)
% integral of the integrand 1/r, through the use of the primitive functions
% prim1, prim2,prim3 and prim4

% AvDiscrGF is to be used in Galerkin formulations. If the mean theorem is
% used, AvDiscrGF can be approximated by the corresponding DiscrGF value

% J. R. Mosig, EPFL Switzerland, 01/06/2023

function [result] = AvDiscrGF(xc,yc,zc,a,b)

zc=zc+eps;
prim1 = @(u,v) u*asinh(v/sqrt(u^2+zc^2))+v*asinh(u/sqrt(v^2+zc^2))...
      - zc*atan(u*v/(zc*sqrt(u^2+v^2+zc^2)));
prim2 = @(u,v) (v*sqrt(u^2+v^2+zc^2)+(u^2+zc^2)*asinh(v/sqrt(u^2+zc^2)))/2;
prim3 = @(u,v) (u*sqrt(u^2+v^2+zc^2)+(v^2+zc^2)*asinh(u/sqrt(v^2+zc^2)))/2;
prim4 = @(u,v) (u^2+v^2+zc^2)^(3/2)/3;

Yuu=(xc-a)*(yc-b)*definite(prim1,xc-a,xc,yc-b,yc)...
    -(yc-b)*definite(prim2,xc-a,xc,yc-b,yc)...
    -(xc-a)*definite(prim3,xc-a,xc,yc-b,yc)...
    +definite(prim4,xc-a,xc,yc-b,yc);
Yud=-(xc-a)*(yc+b)*definite(prim1,xc-a,xc,yc,yc+b)...
    +(yc+b)*definite(prim2,xc-a,xc,yc,yc+b)...
    +(xc-a)*definite(prim3,xc-a,xc,yc,yc+b)...
    -definite(prim4,xc-a,xc,yc,yc+b);
Ydu=-(xc+a)*(yc-b)*definite(prim1,xc,xc+a,yc-b,yc)...
    +(yc-b)*definite(prim2,xc,xc+a,yc-b,yc)...
    +(xc+a)*definite(prim3,xc,xc+a,yc-b,yc)...
    -definite(prim4,xc,xc+a,yc-b,yc);
Ydd=(xc+a)*(yc+b)*definite(prim1,xc,xc+a,yc,yc+b)...
    -(yc+b)*definite(prim2,xc,xc+a,yc,yc+b)...
    -(xc+a)*definite(prim3,xc,xc+a,yc,yc+b)...
    +definite(prim4,xc,xc+a,yc,yc+b);
result=(Yuu+Yud+Ydu+Ydd)/(a*b)^2;
end
```

It is interesting to compare the values of Discrete and Averaged Discrete Green's functions given by these scripts, to foresee the possible differences that could be observed if different MoM approaches (Galerkin, PM, rough approximations based on direct GF values...) are applied to the same problem. This has been done graphically in the paper. Here we complement that information with some numerical values of Ψ, Γ, G for specific cells' positions and considering only unit square cells

$(a = b = 1)$. It is worth recalling that these values correspond directly to the MoM matrix values. For instance, the self-case gives the main diagonal elements; and the interaction between adjacent cells will frequently appear in the elements adjacent to the matrix main diagonal. So, the following table is telling us the differences between MoM matrices in different implementations.

Some possible MoM matrix elements for alternative strategies. Several different positions (xc,yc,zc) of the test cell are considered. The basis cell is always at (0,0,0)

	VALUES			REL. DIFFERENCES (%)		
	GAL (Ψ)	PM (Γ)	GF (G)	Γ vs Ψ	G vs Ψ	G vs Γ
Self case (0,0,0)	2.9732	3.5255	Inf	+18.6	Inf	Inf
Adjacent cells (1,0,0)	1.1121	1.0380	1.0000	-6.6	-10.0	-3.6
Corner-touching cells (1,1,0)	0.7490	0.7247	0.7071	-3.2	-5.6	-2.4
Far away cells (4,0,0)	0.2513	0.2506	0.2500	-0.17	-0.33	-0.17
On top closer cells (0,0,0.1)	2.4674	2.9533	10.0000	+19.7	+305	+239
On top cells (0,0.1)	0.8788	0.9286	1.0000	5.6	13.8	7.7
On top far away cells (0,0,5)	0.1987	0.1933	0.2000	0.3	0.6	0.3

All the analytical values of Γ_{ij} and Ψ_{ij} in the table have been checked by making a rough direct numerical integration of the two-fold integral in (17) and the four-fold integral in (11) using standard quadratures. The results of these quadratures always converge towards the analytical values, although the convergence can be very slow and require a very large number of evaluation points if the basis and test cells are partially or totally overlapping. When the basis and test cells aren't overlapping, the differences between numerical and analytical values remain below 0.1%. But when the basis and test cells are partially overlapping or fully coincident (self-case corresponding to the MoM matrix diagonal), numerical problems will arise, because of the singularities in the integrands, and many simple quadrature schemas will give Inf or NaN results. For the self-case, our analytical expressions are practically unavoidable. But they can also save a lot of computer time when cells are adjacent or close, especially in Galerkin strategies, when the GF needs to be evaluated at least $20^4 = 160'000$ times or more to obtain accurate results.

A warning must be issued in the case of parallel plate problems, where many out-of-diagonal values will correspond to interactions between cells separated by a distance smaller or comparable to the cells' dimensions. In these cases, plain GF values should not be used at all. This fact, evident from the table values, was recognized by Harrington who used a better approximation, replacing the square cells by circular ones of the same area and using the analytical formula for a uniformly charged circular disk [1, eqn. 2.43].

All the above results are for square cells. When very elongated rectangular cells are used, a careful comparison of the associated values must be performed before implementing any approximation.

With the three above MatLab functions, we can now write our Static MoM MatLab code `StaticPlate`, which can solve, with minor modifications, many electrostatic problems involving parallel rectangular metallic plates in free space:

```
% StaticPlate
% Study of the charge distribution in a metallic rectangular plate.

% The rectangle of sides (aside,bside) is divided into MxN square cells.
% Hence, there will be MxN cells with unknown charge values.
% Therefore, the MoM matrix will have (M*N)^2 elements to be computed and
% stored, since no symmetries are considered here.

% Both Galerkin and PM implementations are included.
% They can be called with the MatLab functions StatMoM.

% J.R. Mosig, EPFL Switzerland, June 2023

clear all
% Rectangular plate data: dimensions (meters) of the plate
aside=1
bside=1
% The plate is divided into MxN cells
M=20
N=20
a=aside/M;
b=bside/N;      %  a,b are the cells' dimensions

% 1) A SIMPLE VERSION OF WHAT A GOOD MESHER SOFTWARE SHOULD PROVIDE
% Coordinates (x,y)of all cell centers
% First the x,y coordinates are created as square matrices
% xmat, ymat, zmat since this is natural for a 2D plate.
x=linspace(a/2,aside-a/2,M);
y=linspace(b/2,bside-b/2,N);
[xmat,ymat]=meshgrid(x,y);

% But then,the coordinates are reformatted as 1D-tables (vectors) since
% this is required by the MoM method.
xvec=reshape(xmat,1,M*N);
yvec=reshape(ymat,1,M*N);

% 2) FILLING THE MoM MATRIX
% Here the Green's matrix is filled in an old-fashioned way using a double FOR loop.
% More elegant strategies using the matrix/array operations typical of MatLab
% could be implemented.
% For the MoM matrix elements Galerkin, PM or plain GF values are selected,
% depending on the values of "tresh" and "flagG" in the call to StatMoM

NDIM=M*N       % NDIM is the order of the matrix
tresh=10
```

```
flagG=0
mom=zeros(NDIM,NDIM);
for i=1:NDIM
  for j=1:NDIM
     mom(i,j)=StatMoM(xvec(j),yvec(j),0,xvec(i),yvec(i),0,a,b,tresh,flagG);
  end
end

% 3) COMPUTING THE EXCITATION VECTOR
% Scenario 1):  A constant normalized potential Unorm is imposed on the
% metallic plate. This corresponds to a constant excitation vector "excv"
Unorm=1;
excv=Unorm*ones(NDIM,1);

% Scenario 2):  A point unit charge is placed at point (xq,yq,zq)
%xq=0.5
%yq=0.5
%zq=0.5
%excv=zeros(NDIM,1);
%for i=1:NDIM
%    excv(i)=1/sqrt((xq-xvec(i))^2+(yq-yvec(i))^2+zq^2);
%end

% 4) SOLVING THE LINEAR SYSTEM AND COMPUTING CHARGES AND THE CAPACITANCE
% The solution of the linear system is the array "charge" which contains
% the values of the total charges in each cell (not the charge density!!).
charge=mom\excv;
charge_tot=sum(charge,'all')   % charge_tot is the total charge in the plate
% And in the excitation scenario 1), the normalized capacity is simply:
Capnorm=charge_tot/Unorm
% This value must be multiplied by 4*pi*epsilon0 to obtain the true capacity in farads
```

`StaticPlate` computes the MoM matrix elements calling a single MatLab function `StatMoM` which allows to select either a Galerkin `(AvDiscrGF)` or a Point-Matching strategy `(DiscrGF)` and/or use at will the plain GF approximation.

```
% StatMoM computes the MoM matrix element corresponding to the interaction
% between two parallel xy-cells with identical sizes&orientations and
% centers in (xb,yb,tb) and (xt,yt,zt).
% If the distance between the cells' centers is greater than a threshold
% value given by tresh*max([a b]), then the interaction is approximated by
% the corresponding GF value. Otherwise, Galerkin (AvDiscrGF) values are
% % used if flagG=1 and Point-Matching (DiscrGF) values if flagG=0.

% J.R. Mosig,EPFL, June 2023

function result = StatMoM(xb,yb,zb,xt,yt,zt,a,b,tresh,flagG)
xc=abs(xb-xt);
yc=abs(yb-yt);
zc=abs(zb-zt);
r=sqrt(xc^2+yc^2+zc^2);      % distance between cells' centers
rh=sqrt(xc^2+yc^2);          % horizontal distance between cells' centers
if(rh>tresh*max([a b]))      % a possible criterion to select MoM strategies
```

```
    result=1/r;                % plain Green's function values
else
    if(flagG==1)
        result=AvDiscrGF(xc,yc,zc,a,b);  % Galerkin values
    else
        result=DiscrGF(xc,yc,zc,a,b);    % Point-Matching values
    end
end
```

The MatLab codes have not written searching for optimized performances in terms of code length, computer time and computer memory. And no vectorization has been undertaken. Rather the code writing aims at clarity and simplicity following linearly the mathematical steps in the paper and reproducing in many aspects the way computer codes were written in Harrington times, with nested MatLab loops "`for`", mimicking the "`do`" loops of old Fortran codes.

S6. How Harrington's parallel plate capacitor values have changed with the book edition

Curiously enough, the fig 2.7 of Harrington's book [1], giving the fringing factor of a parallel plate capacitor with square plates is slightly different in the three official editions, Macmillan (1968), Krieger (1982) and IEEE (1993). Out of curiosity, the author of this paper has scanned and digitized the three versions of fig. 2.7 using the free software "Engauge Digitizer" (https://markummitchell.github.io/engauge-digitizer/).

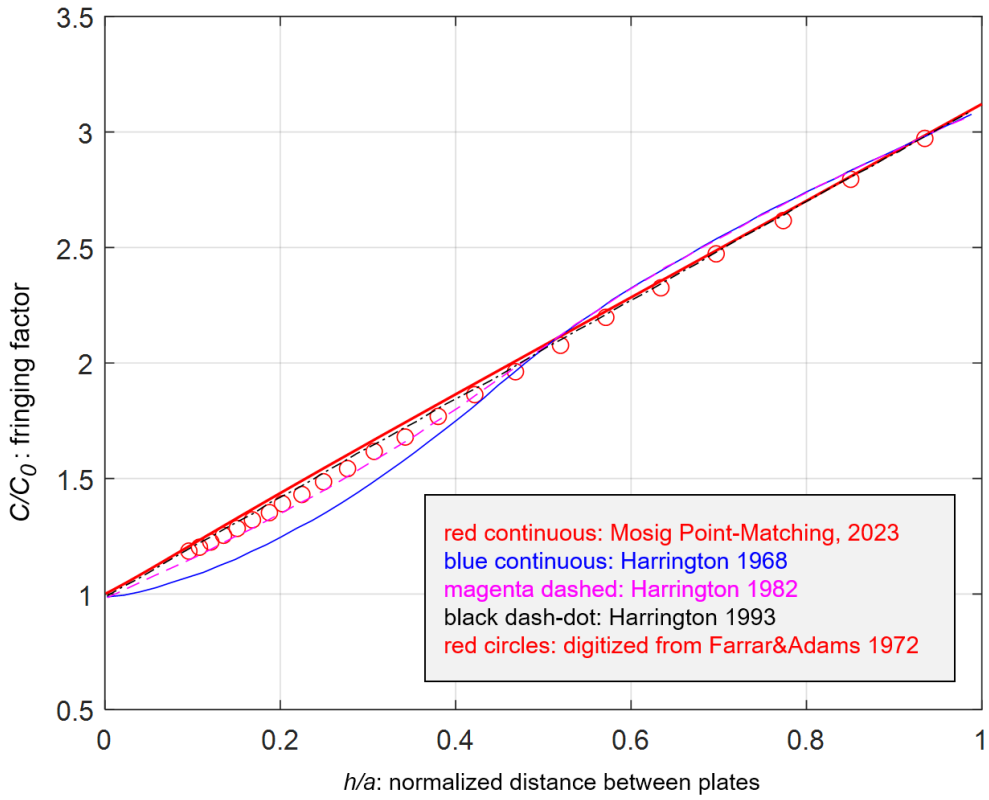

This allowed putting the three curves in the same figure as shown here, where blue continuous is 1968, magenta dashed is 1982 and black dash-dotted is 1993. For comparison purposes, classical

values given by Farrar and Adams in 1972 (also digitized from the original figure) have been added (red circles) as well as the Point-Matching results obtained with the MatLab code in this paper (red continuous line).
It seems that Harrington original 1968 results were not very precise, especially for thin capacitors. Better results were given in the 1982 edition but they had still some errors, especially for thin capacitors. Then, in the 1993 edition, the values were corrected again and they became practically identical to our results. The Farrar&Adams 1972 values confirm this trend as they seem to be in between Harrington 1982 and 1993 values.
With the needed caveat to account for the unavoidable imprecision that comes from digitizing scanned figures taken from papers and books, here are some numerical values for the fringing factor of a square parallel plate capacitor, including the three Harrington editions, the Farrar&Adams papers and the Point-Matching values obtained with `StaticPlate.`

h/a	H-68	H-82	H-93	F&A	PM (M=N=6)
0.2	1.26	1.35	1.43	1.39	1.44
1.0	3.11	3.10	3.11	3.11	3.12